

# RAPID MAGITUDE DETERMINATION FOR TSUNAMI WARNING USING LOCAL DATA IN AND AROUND NICARAGUA

Domingo Jose NAMENDI MARTINEZ\*  
MEE16721

Supervisor: Akio KATSUMATA\*\*

## ABSTRACT

The rapid magnitude determination of an earthquake is at present one of the most important keys to issue tsunami warnings effectively. The goal of this study is to provide an effective magnitude determination method for tsunami warning purpose by analyzing local records of the Central America region. All the data was retrieved from IRIS database from 1995 to 2017 in an epicentral distance range up to 10 degrees and in the magnitudes range between  $M_w$  6 to 7.7. The magnitude range is set so that events which could have tsunami-generating potentials are included. The method utilizes peak displacement amplitudes of different cut-off frequency.

The displacement records are transformed from the original record with a deconvolution filter to correct the instrumental response and high-pass filters. The magnitude is obtained with a simple empirical formula from the peak amplitude. The results obtained using this method scatter considerably from the moment magnitude value of earthquakes in study. This behavior could be caused for the values of coefficients in the formula for amplitude and hypocentral distance. Better coefficients were estimated for the events in this region.

**Keywords:** Tsunami warning, rapid magnitude determination, local seismic records.

## 1. INTRODUCTION

Nicaragua is located in the Central American region and is one of the countries around the Pacific ring of fire. Seismicity of this area is very active due to the interaction between the tectonic plates that converge here (Figure 1). Specifically, on the Pacific coast of Nicaragua, the interaction between the Cocos Plate and the Caribbean Plate are continuously in a process of subduction. This behavior produces a wide variety of earthquakes every year, the biggest magnitude among them is  $M_w$  7.7.

In recent history, in September 1992, an earthquake of magnitude ( $M_w$ ) 7.7 occurred in this region and it induced a tsunami that attacked mainly the Pacific coast of Nicaragua. However, at that time the country had no early warning systems for tsunami. The Nicaraguan Institute of Territorial Studies (INETER) was the organization in charge of managing the national seismic network, however, monitoring was not permanent, and at the time of the earthquake there was no way to determine and to alert the population about a possible tsunami. As a result, the Nicaraguan government has progressively developed the improvement of its alert systems by incorporating equipment and technologies that may be useful for the purposes of monitoring, prevention and issuing alerts if necessary.

---

\* Nicaraguan Institute for Territorial Studies, Geology and Geophysics Department (INETER), Nicaragua.

\*\* Seismology and Tsunami Research Department, Meteorological Research Institute (MRI), Japan.

## 2. DATA

### 2.1. Events selection

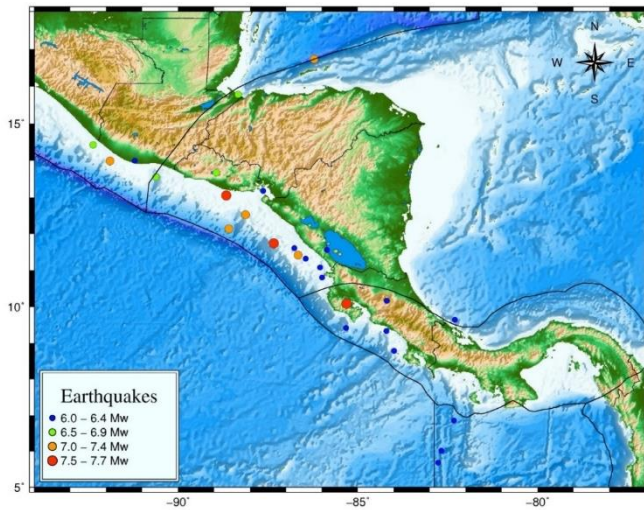


Figure 1. Selected earthquakes, the color and size of dots represent the magnitudes for the events.

We selected 28 events, with magnitudes ( $M_w$ ) between 6 and 7.7 for the study area, from the United State Geological Survey (USGS) catalog. The most important events are those located near the plate boundaries. Figure 1 shows the location of these events; after the selection of events for the analysis, the vertical component of broadband seismic data was retrieved from the Incorporated Research Institute for Seismology (IRIS) database with an epicentral distance  $\Delta \leq 10^\circ$ , by which all Central America regions are covered.

## 3. THEORY AND METHODOLOGY

### 3.1. Data processing

We performed the analyses of the data using SAC software (Goldstein and Snoke, 2003). The correction of instrumental response was the first step applied, and after this, we applied the high pass 3rd order Bessel filter, which is recursive. Several cut-off periods (Table 1) were used in order to measure the maximum displacement ( $A$ ), and this process was repetitive for each event. Figure 2 is an example of one of the events used.

As we described previously, it is necessary to apply the correction of the instrumental response, and the result is shown in Figure 3. The last step is applying the recursive filter and making the measurement of  $A$ . Figure 4 represents an example using the cut-off period of 100 seconds.

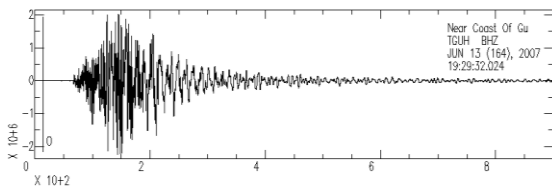


Figure 2. Original waveform of the earthquake near the coast of Guatemala with Magnitude ( $M_w$ ) 6.3 in 1998.

Table 1. Cut-off periods used to measure the maximum displacement  $A$  (m) and coefficients for magnitude determination (Eq. 1, Katsumata *et al.* 2013).

Cut-off periods (sec)	$a$	$b$	$c$
1	1.23	3.48	3.02
2	1.23	3.21	3.17
5	1.23	2.61	4.10
10	1.23	1.99	5.31
20	1.23	1.46	6.39
50	1.23	1.22	6.80
100	1.23	1.24	6.64

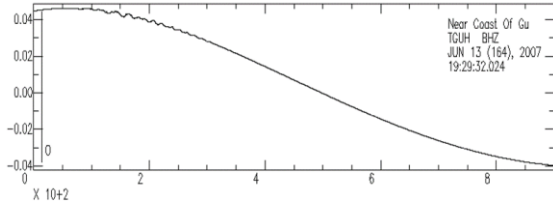


Figure 3. Waveform obtained after application of the deconvolution filter for the correction of instrumental response.

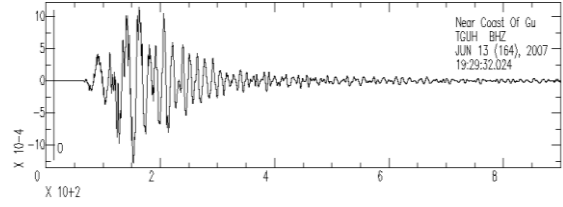


Figure 4. Final waveform obtained by the application of the recursive filter of the 100s cut-off.

Once the measurement of the parameter  $A$  is obtained, we can obtain the magnitude applying the Eq. (1).

$$M = a * \log A + b * \log R + c \quad (1)$$

### 3.2. The high pass filter problem

Long period fluctuations were observed as shown in Figure 5 (case A). A possible reason for this result could be the insufficient resolution of numerical calculation in the SAC program to deal with long period and noise in the data. To avoid this incorrect long period fluctuation, we changed the filter from time domain to frequency domain using pole-zero files of the 3<sup>rd</sup> order Bessel filter (Katsumata, 1993) with transfer command of SAC program. High pass filters are applied now in the frequency domain using a new pole-zero files of Bessel filter. Long period waves were not observed by this method (Figure 5, case B).

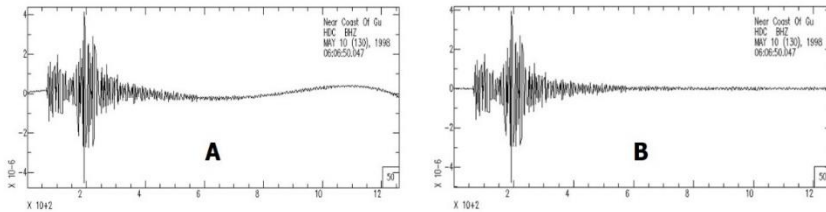


Figure 5. Comparison between the high pass filter (A) and transfer command (B) for the same event described in Figure 2; a cut-off period of 1 second was used.

## 4. RESULTS AND DISCUSSION

From the data processing of 28 selected events, we obtained the average of magnitudes for each event, and for each cut-off period listed in Table 1, Figure 6 shows the differences between the calculated magnitude and  $M_w$  ( $M - M_w$ ) with respect to  $M_w$  from USGS's Catalog.

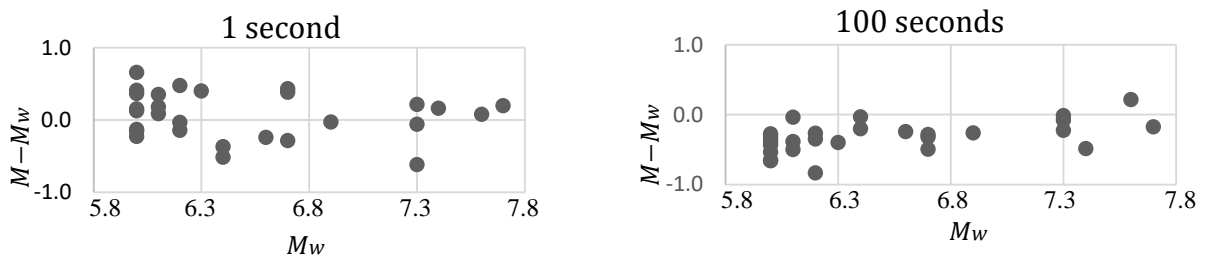
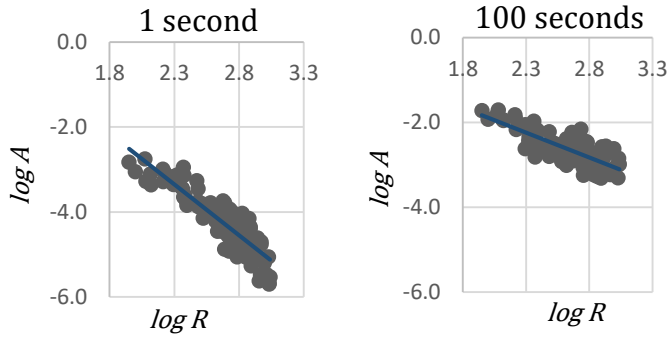


Figure 6. Differences between the calculated magnitude  $M$  (using 1 and 100 seconds) and the moment magnitude. The horizontal axis represents  $M_w$  and the vertical axis represents the average magnitude over stations.

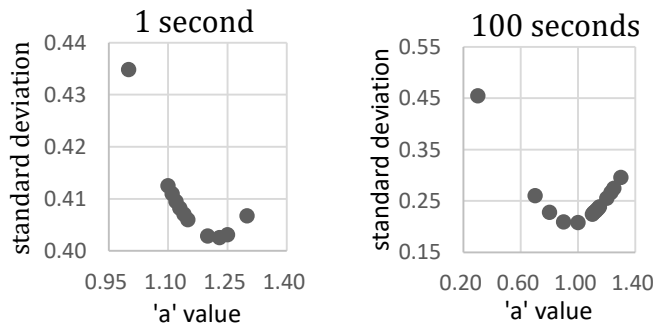
#### 4.1. Coefficients for magnitude determination



The differences between the calculated magnitude are larger than expected, the possible reasons could be inappropriate values of the coefficient in the formula. Figure 7 shows the observed displacement amplitudes with the fitted lines with respect to hypocentral distance. This figure indicates that the coefficient ‘*b*’ for hypocentral distance correction would be good enough to present the attenuation of amplitude along the distance.

Figure 7. Relationship between hypocentral distance and displacement amplitude. The data is shifted in amplitude with the following relation  $\log_{10}R - (7 - M_w)/a$ .

To find a solution, we can make an evaluation of the coefficients of the formula by setting different values to ‘*a*’ and ‘*c*’ and comparing the deviation from  $M_w$ . Figure 8 shows the standard deviation defined by Eq. (2), where  $M$  is the magnitude calculated here,  $M_w$  is the moment magnitude,  $M_{ave}$  is the average of magnitude difference and  $n$  is the number of data set.



$$SD = \sqrt{\frac{\sum\{(M - M_w) - M_{ave}\}^2}{n}} \quad (2)$$

Figure 8. Curve of standard deviation vs ‘*a*’ values, the values selected for the different cut-off periods are showed in Table 2.

The selection of ‘*a*’ was done based on the standard deviation; the value situated at the bottom of the curve is for each case, the optimum, and it provided the best performance in the formula. With the obtained results, we can plot again the magnitude difference ( $M - M_w$ ) with respect to moment magnitude ( $M_w$ ) in Figure 9.

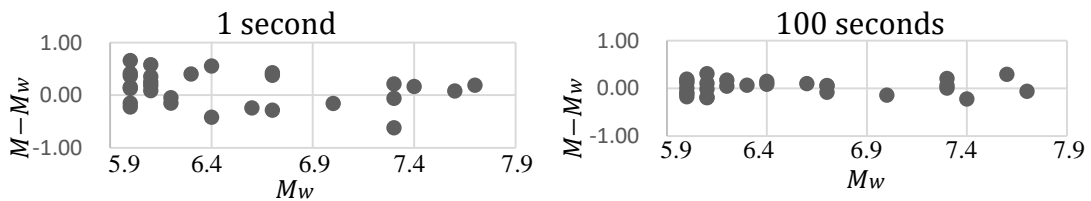


Figure 9. Average between the calculated magnitude  $M$  using the new coefficients, with  $a = 1.23$  for 1, 2, 5,  $a = 1.14$  for 10 seconds and  $a = 0.9$  for 20, 50 and seconds.

Table 2. Final coefficients for the data set.

Cut-off periods (sec)	<i>a</i>	<i>b</i>	<i>c</i>
1	1.23	3.48	2.93
2	1.23	3.21	3.14
5	1.23	2.61	4.16
10	1.14	1.99	5.12
20	0.9	1.46	5.55
50	0.9	1.22	6.10
100	0.9	1.24	6.01

The previous figures (8 and 9) are the results of the setting of the coefficient ‘*a*’ from 1.0 to 1.30 for 1, 2, 5 and 10 seconds while for 20, 50 and 100 seconds the selected ranged was from 0.3 to 1.30. For the case of 1, 2, 5 ‘*a*’ is 1.23, which is the same as in the original formula. However, ‘*c*’ was adjusted based on average difference. In the cases for 20, 50 and 100 seconds, the same value (0.9) is adopted since the same values were obtained for the case of 50 seconds. For 10 seconds the value of 1.14 was selected; this is showed in Table 2, now the differences in the magnitude calculated here are not larger than before. The new coefficients seem appropriate for the formula.

#### 4.2. Time evaluation for magnitude determination

Owing to the simplicity of this method, the time required to calculate the magnitude is around three minutes or less from the origin time (Figure 10). This is good enough for issuing tsunami warnings promptly. For other kinds of magnitudes such as  $M_w$  for example, it takes more time to calculate the

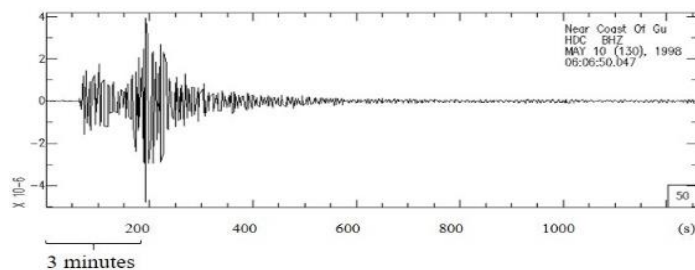


Figure 10. Time when the magnitude could be calculated. The peak amplitude was observed about three minutes after the origin time in this case.

magnitude (more than 5 minutes). This method is applicable for regular earthquakes. However, for tsunami earthquakes such as the Nicaragua earthquake in 1992, this method is not applicable because this method uses only the information of peak amplitude and hypocentral distance.

#### 4.3. The case of Nicaragua earthquake on September 2<sup>nd</sup>, 1992

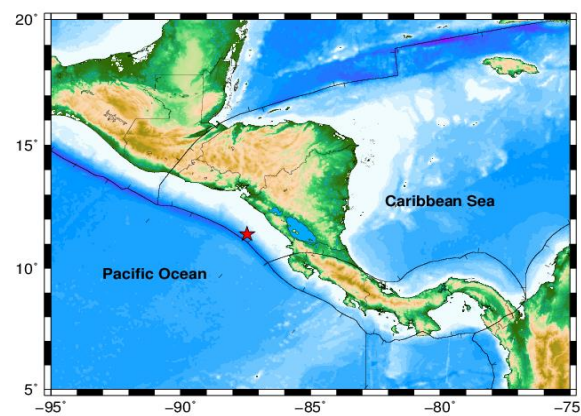


Figure 11. Epicenter location for the Nicaragua earthquake on September 2<sup>nd</sup>, 1992. The red star in the figure represents the epicenter of the Nicaragua earthquake.

We also applied the method to the case of the Nicaragua earthquake in 1992 (Figure 11), which is a typical tsunami earthquake. A tsunami earthquake is considered an event with longer duration compared with normal one (Kanamori, 1972). While the moment magnitude of this event was  $M_w$  7.7, the magnitude calculated was 7.1 using the amplitude of 100 seconds. This is a considerable underestimation. In this case, the data at single station was used, and the epicentral distance is  $15^\circ$ , which is out of the applicable hypocentral distance range. This method was applied using a single station with a location a little out of the applicable distance range of this method ( $\Delta = 10^\circ$ ). Even the condition was not good, this result indicates that this method may underestimate the magnitude of tsunami earthquakes.

## 5. CONCLUSIONS

In this investigation for rapid magnitude determination, we used the vertical component of broadband data retrieved from IRIS database, and we used the USGS's catalog. Twenty-eight events were analyzed using the method developed by Katsumata *et al.* (2013). In measuring the amplitude, long period waves were observed probably due to the insufficient precision of the SAC program. By changing the filter from time-domain to frequency domain, we could get appropriate seismic records.

The results of the magnitude deviate slightly more than expected and were not good enough. It was necessary to change the values of 'a' coefficient for logarithmic amplitude in order to get better fitting between the calculated magnitude and the moment magnitude. After the modification, we found a good correlation between the magnitude calculated in this study and the moment magnitude.

## ACKNOWLEDGEMENTS

I would like to express my sincere gratitude to my supervisor Dr. Katsumata and also to my advisor Dr. Hara for all the effort and support given to me through all of my individual study. To the Japan International Cooperation Agency (JICA), the International Institute of Seismology and Earthquake Engineering – Building Research Institute (IISEE-BRI) and the National Graduate Institute for Policy Studies (GRIPS) for support my scholarship.

## REFERENCES

- Kanamori, H., 1972, Mechanism of tsunami earthquakes, *Phys., Earth Planet Interiors*, 6, 346-359.
- Katsumata, A., 1993, Automated designing of Bessel digital filters, *Quart. J. Seismol.*, 56, 17-34.
- Katsumata, A., H. Ueno, S. Aoki, Y. Yoshida, and S. Barrientos, 2013, Rapid magnitude determination from peak amplitudes at local stations, *Earth Planets Space*, 65, 843-853, doi:10.5047/eps.2013.03.006.
- Goldstein, P., D. Dodge, M. Firpo, Lee Minner, 2003, "SAC2000: Signal processing and analysis tools for seismologists and engineers, Invited contribution to "The IASPEI International Handbook of Earthquake and Engineering Seismology", Edited by WHK Lee, H. Kanamori, P.C. Jennings, and C. Kisslinger, Academic Press, London.
- Web site: Incorporated Research Institute for Seismology (IRIS), Wilber3:  
[http://ds.iris.edu/wilber3/find\\_event](http://ds.iris.edu/wilber3/find_event)
- Web site: United States Geological Survey (USGS): <http://earthquake.usgs.gov/earthquakes/search>